Struct Multidisc Optim 22, 230–239

A simple checkerboard suppression algorithm for evolutionary structural optimization

Q. Li, G.P. Steven, Y.M. Xie

Abstract Checkerboard patterns are quite common in various fixed grid finite element based structural optimization methods. In the evolutionary structural optimization procedure, such checkerboard patterns have been observed under various design criteria. The presence of checkerboard patterns makes the interpretation of optimal material distribution and subsequent geometric extraction for manufacturing difficult. To prevent checkerboarding, an effective smoothing algorithm in terms of the surrounding element's reference factors is proposed in this paper. The approach does not alter the mesh of the finite element model, nor increase the degree of freedom of the structural system, therefore, it does not affect the computational efficiency. To demonstrate the capabilities of this algorithm, a wide range of illustrative examples are presented in this paper.

Key words finite element analysis, structural optimization, checkerboard patterns, multiple criteria

1 Introduction

Checkerboard patterns refer to the phenomena of alternating presence of solid and void elements ordered in a checkerboard like fashion (Sigmund and Petersson 1998). This pattern can be commonly produced in various finite element based structural optimization processes. Such shapes and topologies with checkerboard patterns may be unacceptable in practice. For this reason, the solutions to the checkerboard problems have attracted considerable attention in the past several years. The previous researchers have devoted their efforts on two significant aspects:

1. the cause of checkerboard formation, and
2. the suppression techniques of checkerboard patterns.

To identify the formation mechanism of the checkerboard, Bendsøe *et al.* (1993) described a four-node displacement model with piecewise constant density field through a patch test, in which an effective super element is introduced to the finite element formulation. The investigation by Jog *et al.* (1994) showed that the choice of basis functions for both displacement and density fields is critical in optimization, when using the homogenization method. This means that the combination of high order displacement model (8-node) with a low order bilinear density field cannot ensure a stable solution. Diaz and Sigmund (1995) used a patch test of four-node elements to indicate that, in a compliance minimization design, the checkerboard patterns appear to be locally stiffer than any other distribution of the two constituent materials. Similarly, theoretical framework of Jog and Haber (1996) further demonstrated that the cause of checkerboard formation is numerical rather than physical in nature. Above work has significantly contributed to the understanding of the checkerboard formation in the stiffness based optimization.

Although the origin of checkerboard patterns is still not fully understood, in particular for various design optimization criteria, it is likely to be related to the finite element approximation. From this point, various interpretation schemes and suppression approaches have been proposed. Diaz and Kikuchi (1992) showed that finer checkerboard patterns could approach to solid material with half thickness in the natural frequency optimization. This provided an intuitive interpretation to checkerboard patterns, but the topological implication becomes unclear to a certain extent. To improve the interpolation accuracy of basis functions, one of the approaches suggested is to use higher order elements. The investigation

Received December 22, 1999
Revised manuscript received March 23, 2000

Q. Li[1], G.P. Steven[2], Y.M. Xie[3]

[1] Department of Aeronautical Engineering, University of Sydney, NSW 2006, Sydney, Australia
[2] School of Engineering, University of Durham, Durham DH1 3LE, UK
e-mail: grant.steven@durham.ac.uk
[3] Faculty of Engineering and Science, Victoria University of Technology, P.O. Box 14428, Melbourne City MC, VIC 8001, Australia
e-mail: grant@aero.usyd.edu.au

reported by Rodrigues and Fernandes (1995) successfully removed checkerboarding in thermoelastic optimization problems. However, the degrees of freedom of the structural system are greatly expanded with a commensurate increase in the computational cost. To overcome this computational difficulty introduced by the high order elements, various modification algorithms for design variable and response parameters are developed for the four-node element. Bendsøe *et al.* (1993) suggested a patch modification technique inspired by the similar problems in Stokes flow. But this did not always entirely eliminate checkerboarding in topology optimization. Based on filtering techniques from image processing, Sigmund and Petersson (1998) developed a checkerboard prevention filter by a weighted average over element itself and its eight direct neighbors. Following this line, Youn and Park (1997) as well as Swan and Kosaka (1997) also employed neighbouring elements to redistribute elemental density, which promptly improves the subiteration results of the design variables. By relaxing the slope constraints of density function, Zhou *et al.* (2000, 2001) developed a density control algorithm into the commercial structural optimization package Altair OptiStruct. These algorithms have been proven effective in seeking compliance minimization problems while not increasing the computational cost greatly.

In the evolutionary structural optimization (ESO) method (Xie and Steven 1993, 1997), checkerboard patterns can also be observed in various four-node element based design problems. With the ESO method, material alternation (increase or reduction) of an element is determined in terms of its relative reference level. In this sense, the appearance of checkerboard patterns reflects an improper estimation on the elemental evolutionary criterion. It is believed that such a situation is also caused by the poor numerical behavior of four-node elements in 2D models. The numerical experiments conducted by Manickarajah *et al.* (1998a) showed that the use of higher order elements, e.g. 8-node elements, can significantly reduce the occurrence of checkerboarding. But this was not an appropriate solution due to the considerable increase in computational time. Similarly to the approach of Haber *et al.* (1996), Kim *et al.* (2001) developed an algorithm of Intelligent Cavity Creation (ICC), in which the checkerboarding patterns (with numerous cavities) can be eliminated through controlling the number of cavities in the final topology. In this paper, to improve the estimation quality of elemental sensitivity or reference level in low order elements, a weighted average algorithm is developed to balance the *over* or *under* evaluation of the evolution criteria. Although theoretical work is still required to fully understand the formation mechanism of checkerboarding, in particular, with different design criteria, this paper focuses on demonstrating the effectiveness of the proposed elimination algorithm. For this purpose, a variety of demonstrative examples are presented in this paper, which include 2D/3D regions, topology/shape, single/multiple components and single/multiple load cases with single/multiple design criteria of structural stiffness, natural frequency, buckling load, thermoelastic displacement, heat flux density and stress level. It is found that this approach is easy to be implemented into various criteria and works equally well in 2D and 3D structures.

2
Brief description of evolutionary design criteria

Evolutionary structural optimization aims at modifying (removing or adding) material distribution to seek one or several specific design objectives. With finite element analysis, the material removal or addition is carried out on the basis of elements. In the ESO method, an element's alteration is determined in terms of its effect on the design objective. For this reason, this section will briefly describe the design criteria for various situations that are prone to form the checkerboard patterns.

2.1
Stiffness based criterion

It is known that, removal or addition of material from element i will lead to the change (sensitivity number) in structural mean compliance or strain energy by

$$\alpha_i = \Delta C = \frac{1}{2}\mathbf{f}^T \Delta \mathbf{u} = \frac{1}{2}\mathbf{u}_i^T \Delta \mathbf{K}_i \mathbf{u}_i \,, \tag{1}$$

where $\Delta \mathbf{K}_i$ denotes the change in the stiffness matrix of candidate element i when reducing or increasing its material (Chu *et al.* 1998). This provides an inverse measure in the change of structural overall stiffness. To seek the stiffest design, material should be gradually removed from the lowest sensitivity elements or added onto the highest sensitivity elements.

2.2
Natural frequency criteria

In order to avoid severe induced vibration, it is often necessary to produce a design that shifts the fundamental (first) frequency or several of the lower frequencies of the structure away from the specific frequency range of the dynamic loading. To estimate the effect of material removal and addition of an element on the natural frequencies, a frequency sensitivity can be derived as (Xie and Steven 1996, 1997; Zhao *et al.* 1997)

$$\alpha_i = \Delta \omega_j = \frac{1}{m_j}\mathbf{u}_{ij}^T \left(\omega_j^2 \Delta \mathbf{M}_i - \Delta \mathbf{K}_i\right) \mathbf{u}_{ij} \,, \tag{2}$$

where $m_j = \mathbf{u}_{ij}^T \mathbf{M} \mathbf{u}_{ij}$ gives modal mass, $\mathbf{u}_{ij}$ denotes the corresponding eigenvector of element i and ω_j the j-th

natural frequency. To most effectively increase or reduce a specific frequency, material should be removed from either those elements with the most highly positive or the most highly negative sensitivities, respectively.

2.3 Buckling load criterion

To increase the buckling resistance of a structure, a sensitivity number of the critical value of the load factor λ with respect to the decrease or increase in candidate element material can be evaluated as (Manickarajah *et al.* 1998a,b)

$$\alpha_i = \Delta\lambda_j = \mathbf{u}_{ij}^T \left(\Delta\mathbf{K}_i - \lambda_j \Delta\mathbf{K}_{g,i}\right) \mathbf{u}_{ij} \,, \tag{3}$$

where λ_j denotes the j-th eigenvalue and $\mathbf{u}_{ij}$ the corresponding eigenvector for element i, $\Delta\mathbf{K}_{g,i}$ represents the change in the geometric stiffness matrix of the candidate element i. As with the vibration and from the definition of the sensitivity number, it is clear that to raise the buckling load factor it will be most effective to increase the material of elements with the highest sensitivity, or reduce material from those with the lowest sensitivity.

2.4 Thermoelastic displacement criterion

To control the deformation in thermoelastic structure, a displacement sensitivity number, which indicates the nodal displacement change along a specific direction (e.g. the j-th d.o.f.), can be evaluated as (Li *et al.* 1999b)

$$\alpha_i = \Delta u_j = \mathbf{u}_{ij}^T \cdot \Delta\mathbf{f}_{i,\mathrm{th}} - \mathbf{u}_{ij}^T \cdot \Delta\mathbf{K}_i \cdot \mathbf{u}_i \,, \tag{4}$$

where $f_{i,\mathrm{th}}$ represents the change in the elemental equivalent thermal nodal force under a certain differential of the temperature $\Delta T = (T - T_{\mathrm{ref}})$ due to removing or adding material in candidate element i, $\mathbf{u}_{ij}$ denotes the displacement entries of candidate element i from the solution of virtual system $\mathbf{K}\mathbf{u}_j = \mathbf{f}_j$ (the j-th d.o.f. of $\mathbf{f}_j$ is equal to unity and all the others are equal to zero). The thermoelastic sensitivity number α_i can be positive or negative, which implies that the displacement component U_j may increase or decrease when there is a change in the material of element i.

2.5 Thermal stress and heat flux criteria

In a thermal environment, a structure usually experiences heat flux and thermal stress. To estimate the relative efficiencies of material usage of candidate element i, two dimensionless factors, $\alpha_\sigma^i = \sigma_{\mathrm{vm}}^i / \sigma_{\mathrm{vm}}^{\max}$ and $\alpha_f^i = J_{\mathrm{vm}}^i / J_{\mathrm{vm}}^{\max}$ (Li *et al.* 1999a,c), are defined. From the viewpoint of isostrength and iso-flux density, the elemental overall contribution to such two criteria can be evaluated in terms of the weighted average scheme as

$$\alpha_i = w_\sigma \alpha_\sigma^i + w_f \alpha_f^i \,, \tag{5}$$

where w_σ and w_f denote weighting coefficients for thermal stress and heat flux criteria, respectively, which satisfy $w_\sigma + w_f = 1$. To achieve as uniform an efficiency of material usage as possible, it is logical to gradually remove the elements with the lowest overall efficiency from the structure (Li *et al.* 1999c).

2.6 Stress based criterion

Stress is an important indication of material usage of a structure. Ideally the stress in every part of a structure is near the same safe level. This concept leads to a rejection or addition criterion based on elemental stress level, where lowly (or highly) stressed material is assumed to be under-utilized (or over-utilized) and is to be removed (or added) in the structures. As a result, the level of elemental von Mises stress is regarded as the criterion to decide the material removal (Xie and Steven 1993) or addition (Querin *et al.* 1998) as

$$\alpha_i = \sigma_{\mathrm{vm}} = \left(\mathbf{u}_i^T \mathbf{B}^T \mathbf{Z} \mathbf{B} \mathbf{u}_i\right)^{\frac{1}{2}} \,, \tag{6}$$

where $\mathbf{Z} = \mathbf{D}^T \mathbf{T} \mathbf{D}$, $\mathbf{T}$ is the coefficient matrix of the von Mises quadratic form, $\mathbf{u}_i$ represents elemental displacement vector, and $\mathbf{D}$ and $\mathbf{B}$ denote the elastic and stress-strain matrices, respectively. Through progressively removing lowly stressed material (strongest) or shifting material from lowly stressed elements (strongest) to highly stressed ones (weakest), the stress distribution or structural strength over the design domain evolves towards more uniform (Xie and Steven 1997).

3 Suppression algorithm of checkerboard patterns

The ESO procedure is directly driven by the elemental reference factor as outlined in the preceding section. In a continuum structure which is discretized using low order bilinear (2D) or trilinear (3D) finite elements, the reference factors could become C^0 discontinuous across element boundaries. In other words, the C^1 discontinuity of interpolation function between adjacent elements leads to the resulting reference sensitivity factors, as defined in (1–6), varying in a stepwise manner. In evolutionary structural optimization, the evidence of alternative solid and void patterns supports an explanation that the design criterion is either overestimated or underestimated alternately (Jog and Haber 1996). To correct such errors caused by finite element approximation, an intuitive smoothing technique can be in-

troduced. In brief, this procedure consists of two basic steps:

1. Calculate the reference factor at each node by averaging the element ones connecting to this node as

$$\alpha_k = \frac{\sum_{i=1}^{\mathrm{ne}} V_i \alpha_i}{\sum_{i=1}^{\mathrm{ne}} V_i}, \tag{7}$$

where ne denotes the total number of elements connected to the k-th node, α_i and V_i the reference factor and volume of the i-th connection element, respectively.

2. Calculate the smoothed reference factor of the candidate element (e) by averaging all nodal ones of this element as

$$\alpha_e = \frac{1}{V_e} \int_{V_e} \mathbf{N}_k \alpha_k \, \mathrm{d}V, \tag{8}$$

for regular square elements, simply,

$$\alpha_e = \frac{1}{n} \sum_{i=1}^{n} \alpha_k, \tag{9}$$

where $\mathbf{N}_k$ is the vector of shape function of the candidate element e, n denotes the node number of this element, V_e the elemental volume.

This is viewed as a first-order smoothing technique, where the reference factor of the candidate element is calculated from its own and those directly attached elements (e.g. Fig. 1a). When necessary, a second-order smoothing approach may be applied, in which the smoothed reference factors are smoothed further. In this case, the candidate element itself as well as the first-layer and the second layer of surrounding elements are involved, as in Fig. 1b.

From such a two-step procedure, the smoothed reference factor of element e can be consequently formulated as

$$\alpha_e = \frac{\sum_{i=1}^{m} w_i V_i \alpha_i}{\sum_{i=1}^{m} w_i V_i}, \tag{10}$$

where m is the total number of all involving elements and w_i represents filter parameter, which usually satisfies

$$\sum_{i=1}^{m} w_i = 1. \tag{11}$$

Typically, for the uniform four-node square elements, the filter parameter w_i ($i = 1, 2, \ldots, m$) is given in Figs. 1a and 1b for the first- and the second-order filters, respectively. It is clear that the first-order scheme lays more emphasis on the candidate element itself (25%) than the second-order scheme does (14%). Under many circumstances, seriously checkerboarding often reflects that the reference level is severely under or over evaluated. For this reason, the second-order scheme can provide more correction to the numerical instabilities.

	1	2	1	
	2	4	2	
	1	2	1	

(a) The weighting coefficient $16w_i$ for the first order smoothing scheme

	1	4	6	4	1
	4	16	24	16	4
	6	24	36	24	6
	4	16	24	16	4
	1	4	6	4	1

(b) The weighting coefficient $256w_i$ for the second order smoothing scheme

Fig. 1 The weighting coefficients for checkerboard filter

4 Illustrative examples

To demonstrate the checkerboard suppression technique, a wide range of illustrative examples is presented with 2D quadrilateral or 3D brick element meshes, under different design criteria and using different approaches to material modifications (element elimination or thickness variation).

4.1 Example of 2D stiffness criterion

In stiffness based ESO solutions, different levels of the checkerboard phenomena can be observed in various

examples, in which four node elements are used (refer to Chu *et al.* 1998; Xie and Steven 1997). According to the proof by Jog *et al.* (1994), the choice of basis functions for displacement field is critical to achieve a stable solution in stiffness based optimization. Diaz and Sigmund (1995) also show that artificially high stiffness could account for the formation of checkerboard patterns. In this example, when the smoothing scheme is not used, a cantilever structure within the design domain of 510×210 mm (modeled by 51×21 four-node elements), as given in Fig. 2, does suffer serious checkerboarding as Fig. 2a.

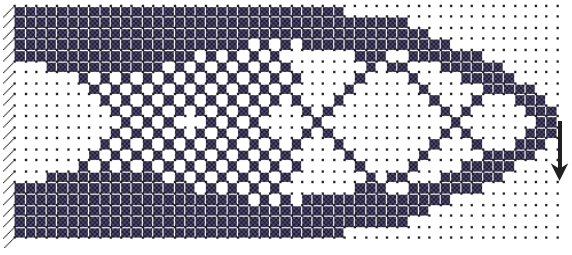

(a) Solution without checkerboard suppression ($V/Vo \approx 45\%$)

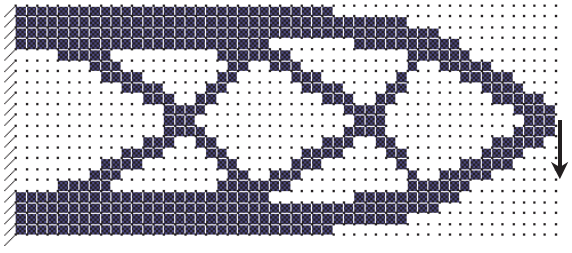

(b) ESO with checkerboard suppression ($V/Vo \approx 45\%$)

Fig. 2 Checkerboard suppression for stiffness criterion

In continuum structures, the density of strain energy is a continuous function. It is found that, however, the energy density or stiffness sensitivity number becomes stepwise in finite element analysis as (1), which experiences discontinuity across elements (Chu *et al.* 1998). This means that the enhancement of the continuity of sensitivity numbers across elements can improve the stability of the solution. As a result, when the proposed smoothing scheme is employed, the checkerboard patterns are completely suppressed from the cantilever structure in this example, as shown in Fig. 2b.

4.2 Example of frequency minimization criterion

In some structures, it is necessary to control the fundamental natural frequency. For this purpose, vibration sensitivity analysis as (2) is needed prior to element removal. In this example, a cantilever structure with the dimension of $300 \times 200 \times 10$ mm is meshed by 30×20 four node elements, where the material properties of Young's modulus 200 GPa, Poisson's ratio 0.3 and density 7.8×10^{-9} Tonne/mm^3 are taken. The potential applied vibration source, such as motor with a certain frequency of operation, is represented in a lumped mass of 10 kg (Zhao *et al.* 1997) at the free end of the structure as illustrated in Fig. 3a.

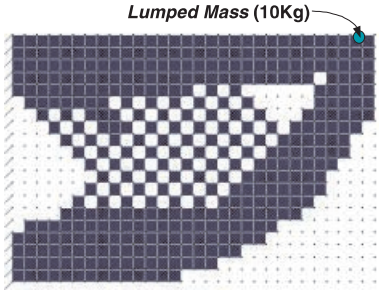

(a) Without checkerboard suppression ($\omega = 82.7 rad/s$, reduced from the initial frequency $\omega = 91.7 rad/s$)

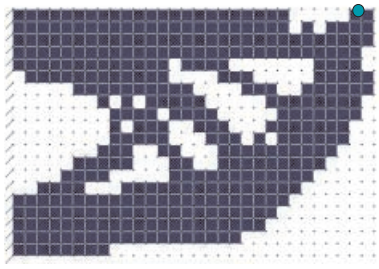

(b) With 1st order filter ($\omega = 81.3 rad/s$)

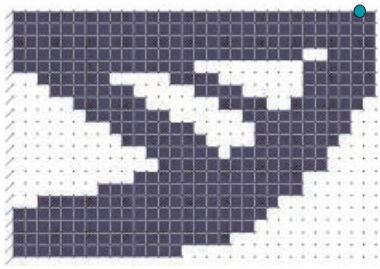

(c) With 2nd order filter ($\omega = 80.5 rad/s$)

Fig. 3 Checkerboard suppression for fundamental frequency minimization ($V/V_0 = 65\%$)

As with the static stiffness optimization, checkerboard patterns can be clearly observed in dynamic optimization as shown in Fig. 3a. However, as opposed to the previous stiffness design example, the first-order filter does not fully remove the checkerboard, as displayed in Fig. 3b. For this reason, the second-order smoothing scheme is required. A checkerboard free topology results from the second-order filter as Fig. 3c. It is worth noting that the

use of the second-order filter does not greatly increase computation cost. Thus it provides a convenient and effective tool capable of dealing with even more stubborn checkerboard phenomena.

Under the first-order filter, the failure to achieve a stable solution may indicate that this correction is not enough to improve the smoothness of frequency sensitivity number across elements. However, this may not always happen and in practice the decision to advance to the second-order smoothing scheme may well be problem dependent.

4.3 Example of buckling load maximization criterion

In the previous topology designs, material removal is carried out through element deletion (so called hard-kill), in which the presence or absence of an element itself is considered as the design variable. Such a discrete optimization algorithm may cause further discontinuity in sensitivity numbers. To improve the continuity of ESO algorithm itself, one may wish to remove material from elements in a stepwise manner (also called morphing ESO). The numerical investigations conducted by Chu *et al.* (1998), Manickarajah *et al.* (1998a,b) explored that this strategy, but do not appear to help suppress checkerboarding. The current example is employed to deal with checkerboard thickness distribution with a buckling load maximization criterion. In this example, a simply supported square plate is subjected to constant uniaxial load analyzed (Manickarajah *et al.* 1998b). The upper and lower bounds of thickness variables are set for $\overline{t} = 20\,\text{mm}$ and $\underline{t} = 10\,\text{mm}$, between which nine selectable discrete thicknesses are given as shown in the thickness legend of Fig. 4.

As shown in Fig. 4a, four-node elements do cause checkerboarding thickness allocation under the buckling criterion, where the thickness evolves to an alternating pattern at either the upper bound $\overline{t}$ or the lower bound $\underline{t}$. Investigation by Manickarajah *et al.* (1998b) has shown that such a checkerboarding thickness allocation does not achieve the desired result when compared to non-checkerboarding equivalent benchmarks. To improve the numerical accuracy and stability, the problem was reanalyzed using the 8-node isoparametric elements (Manickarajah *et al.* 1998a). As expected, the checkerboarding was completely eliminated from the design. This indicates that the higher order elements did improve the numerical stability as proven by Jog and Haber (1996) in stiffness based criterion. But the use of high order elements considerably increases the computational cost (by five times in this specific example). For this reason, the proposed smoothing filter is switched on to a FEA model consisting of four-node elements. The result of smoothly varying thickness distribution (Fig. 4c) shows a close resemblance to the 8-node one (Fig. 4b). With this result it can be argued that the efficacy of the smoothing algorithm works correctly.

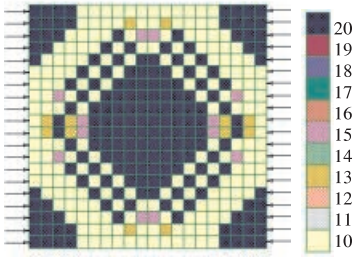

(a) 4 node elements without checkerboard suppression ($N_{cr} = 872.9\text{kN/m}$)

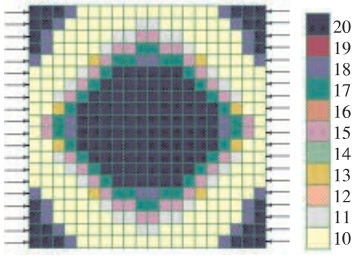

(b) 8-node elements without the filter ($N_{cr} = 826.1\text{kN/m}$)

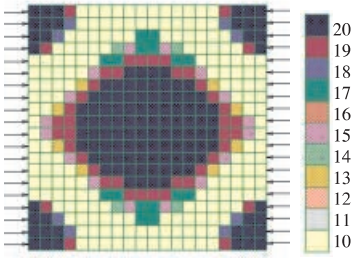

(c) 4-node with the 1st order filter ($N_{cr} = 831.1\text{kN/m}$)

Fig. 4 Checkerboard suppression for buckling resistance criterion

4.4 Example of displacement minimization for thermoelasticity

To extend the capabilities of the ESO morphing algorithm, a thickness based topological design is conducted in this example. A design is sought to minimize the downward displacement in the mechanical loading point on the bottom edge of the thermoelastic region (refer to Li *et al.* 1999b), where the elemental thermal displacement sensitivity with respect to the elemental thickness, as (4), is calculated. To capture topology features, the lower bound of the design variables (elemental thickness) is assigned to a value so much smaller than the upper bound,

e.g. 1% as the thickness legend in Fig. 5. This ensures that the resulting variable thickness design has topology significance.

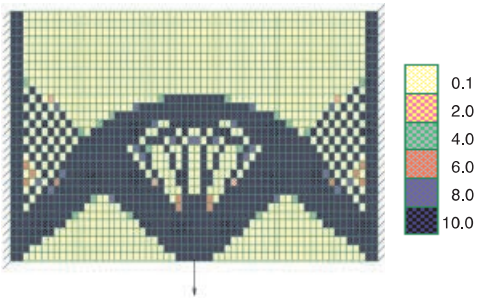

(a) ESO without checkerboard suppression

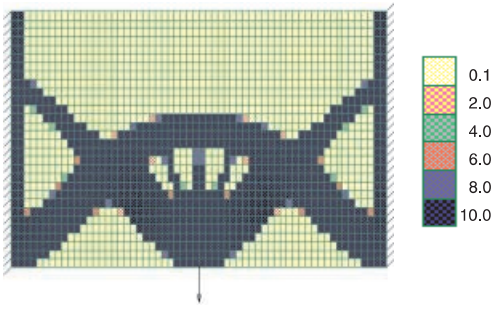

(b) ESO with checkerboard suppression

Fig. 5 Checkerboard suppression for 2D thermoelastic displacement criterion ($V/V_0 = 40\%$, $\Delta T = 1\,^{\circ}\mathrm{C}$)

In addition to the instability of the four-node element itself, the effect of equivalent nodal thermal loading further exacerbates the tendency to numerical in-balance during the thermoelastic optimization processes, thus the checkerboard appearance becomes more prevalent (Rodrigues and Fernandes 1995; Sigmund and Torquato 1997). As with the Homogenization method, the ESO method is also prone to produce a checkerboard pattern as shown in Fig. 5a (Li *et al.* 1999b). In the references (Rodrigues and Fernandes 1995), the numerical instabilities of checkerboard appearances were removed by using the 9-node elements. The checkerboarding regions were consequently switched to an intermediate density material, for which the topology implications are still unclear. Similarly to the use of 8-node elements in the previous example, the drawback of this approach is that the computational efficiency is remarkably reduced because the degrees of freedom of the model are greatly increased. Also, a re-meshing process may be needed to transform four-node elements to 9-node ones.

To overcome these difficulties, the first-order smoothed sensitivity number is employed with the four-node elements. It is found that this successfully prevents checkerboard patterns appearing, as observed in Fig. 5b. The central region near the mechanical loading evolves to a local Michell type structure, which is more acceptable than the intermediate density distributed material. Therefore, the high computational efficiency and the distinct topological definition further demonstrate the effectiveness of the proposed suppression algorithm.

4.5 Example of multiple thermal criteria

The examples in the foregoing subsections show the formation of checkerboarding in various single optimum objectives. Indeed, the checkerboard patterns can also be observed in the designs with multiple criteria. In this example, a printed circuit board (PCB) substrate with the pure thermal loading generated from

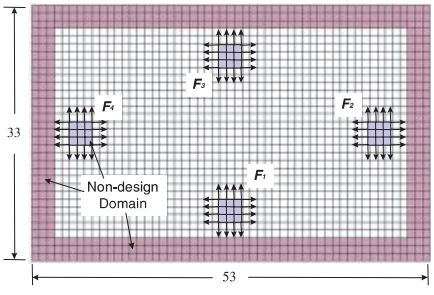

(a) Design model of PCB substrate

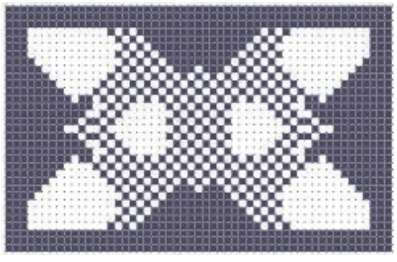

(b) Without checkerboard suppression

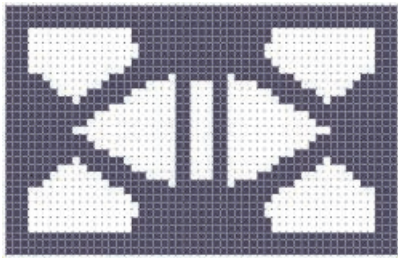

(c) The second order smoothing scheme

Fig. 6 Checkerboard suppression for multiple thermal criteria ($V/V_0 = 60\%$)

four major electronic elements is designed as illustrated in Fig. 6a (refer to Li *et al.* 1999a,c). To seek a fully stressed and evenly fluxed design over the region, the weighted average scheme is used to estimate the elemental overall contribution to strength and thermal criteria as (5).

When there is no checkerboard suppression scheme used, notable checkerboarding can be seen in the central region in Fig. 6b. This is caused by an incorrect estimation of elemental thermal stress level and flux density over this area. When the first-order suppression scheme is set up, the checkerboarding is notably reduced but still present. When the second-order suppression scheme is employed, a good topology is obtained as shown in Fig. 6c, in which the topological layout, as displayed in Fig. 6b has a reasonable physical interpretation.

4.6 Example of 3D von Mises stress criterion

Traditionally, investigations in structural optimization mainly focus on 2D elasticity with a single component (Bendsøe 1995; Rozvany *et al.* 1995; Xie and Steven 1997). This example is presented herein to incorporate 3D objects composed of the two components under multiple load cases, where Components A and B are connected by a number of candidate connection elements as separately illustrated in Fig. 7. In the evolution process, both the connection elements and the component elements are allowed to be removed. In the finite element analysis, 8-node brick elements are used and two load cases are applied at the free end of the cantilever system as shown in Fig. 7. To seek a fully stressed design, the inefficient material that is indicated by elemental von Mises stress level (6) is progressively removed from the structure so that the stress distribution in the remaining structure evolves towards a more uniform level (Xie and Steven 1993, 1997).

When the smoothing filter is turned off, a typical checkerboard pattern can be observed in the central region in Component A as shown in Fig. 8a. This provides an evidence that checkerboard pattern also appears in the 3D 8-node brick elements, where a trilinear displacement field (subject to C^0 continuity) is formulated. In such elements, the level of elemental von Mises stress varies in a stepwise manner from element to element. When the smoothing scheme is switched on, such a discontinuity of stress distribution can be significantly

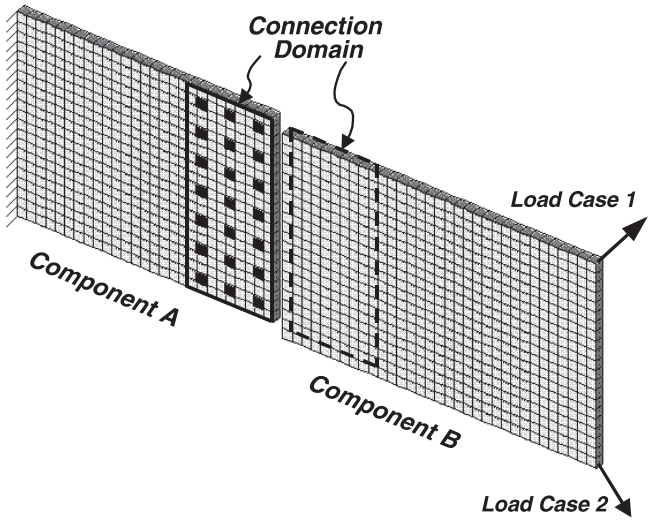

Fig. 7 Design model for 3D multiple components and multiple load cases

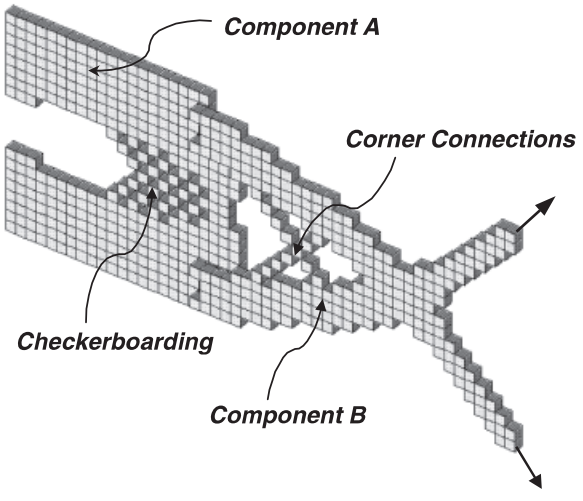

(a) Without checkerboard suppression

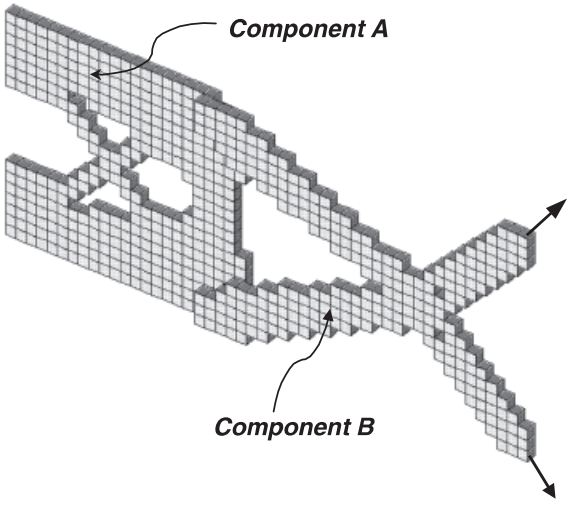

(b) With checkerboard suppression

Fig. 8 Checkerboard suppression for 3D eight node brick elements ($V/V_0 \approx 48\%$)

reduced. As a result, the checkerboard pattern is substituted with a cross truss of Component A as shown in Fig. 8b. In addition, the pattern of the corner connecting elements in Component B (Fig. 8a), which is usually viewed as a by-product resulting from checkerboarding, has also been filtered from the optimal design (Fig. 8b).

5 Concluding remarks

To deal with the checkerboard phenomena, a simple and effective smoothing algorithm involving an element's evolution criterion has been proposed. The approach does not alter the mesh of the finite element model, nor increases the degrees of freedom of the structural system, therefore, it does not affect the computational efficiency. This is an advantage over the use of high order element approaches.

To demonstrate the capabilities of the proposed smoothing filter, this paper has presented a wide range of illustrative examples. These examples increase our understanding in the formation of checkerboard patterns under one or several design criteria such as stiffness, natural frequency, von Mises stress, thermal displacement, buckling load and heat flux. At the same time, the examples present the solutions to a variety of optimal problems such as single or multiple design criteria, single or multiple components, single or multiple load cases, 2D or 3D, and topology or size designs.

Acknowledgements The research was funded by Australian Research Council under the Large Grant Scheme. During the study, the first author was supported by the Australian Postgraduate Award and an Aeronautical Engineering Scholarship at The University of Sydney.

References

Bendsøe, M.P. 1995: *Optimization of structural topology, shape, and material*. Berlin, Heidelberg, New York: Springer

Bendsøe, M.P.; Diaz, A.; Kikuchi, N. 1993: Topology and generalized layout optimization of elastic structures. In: Bendsøe, M.P.; Mota Soares, C.A. (eds.): *Topology design of structures*, pp. 159–205. Dordrecht: Kluwer

Chu, D.N.; Xie, Y.M; Steven, G.P. 1998: An evolutionary structural optimization method for sizing problems with discrete design variables. *Comp. & Struct.* **68**, 419–431

Diaz, A.R.; Kikuchi, N. 1992: Solutions to shape and topology eigenvalue optimization problems using a homogenization method. *Int. J. Numer. Meth. Engrg.* **35**, 1487–1502

Diaz, A.; Sigmund, O. 1995: Checkerboard patterns in layout optimization. *Struct. Optim.* **10**, 40–50

Haber, R.B.; Jog, C.S.; Bendsoe, M.P. 1996: A new approach to variable-topology shape design using a constant on perimeter. *Struct. Optim.* **11**, 1–12

Jog, C.S.; Haber, R.B. 1996: Stability of finite element models for distributed-parameter optimization and topology design. *Comp. Meth. Appl. Mech. Engrg.* **130**, 203–226

Jog, C.S.; Haber, R.B.; Bendsoe, M.P. 1994: Topology design with optimization, self-adaptive material. *Int. J. Numer. Meth. Engrg.* **37**, 1323–1350

Kim, H.; Querin, O.M.; Steven, G.P.; Xie, Y.M. 2001: A method for varying the number of cavities in an optimized topology using evolutionary structural optimization. *Struct. Optim.* (to appear)

Li, Q.; Steven, G.P.; Querin, O. M; Xie, Y.M. 1999a: Shape and topology design for heat conduction by evolutionary structural optimization. *Int. J. Heat Mass Trans.* **42**, 3361–3371

Li, Q.; Steven, G.P.; Xie, Y.M. 1999b: Displacement minimization of thermoelastic structures by evolutionary thickness design. *Comp. Meth. Appl. Mech. Engrg.* **179**, 361–378

Li, Q.; Steven, G.P.; Querin, O.M.; Xie, Y.M. 1999c: Evolutionary optimization for conceptual design in thermal environment. In: Toropov, V.V. (ed.): *Engineering design optimization*, pp. 249–256. MCB University Press

Manickarajah, D.; Xie, Y.M.; Steven, G.P. 1998a: Elimination of checkerboard patterns from plate buckling optimum designs. In: Steven, G.P.; Querin, O.M.; Guan, H.; Xie, Y.M. (eds): *Proc. Australasian Conf. on Structural Optimisation* (held in Sydney, February 11–13), pp. 525–532

Manickarajah, D.; Xie, Y.M.; Steven, G.P. 1998b: An evolutionary method for optimization of plate buckling resistance. *Finite Elements Analysis & Design* **29**, 205–230

Querin, O.M.; Steven, G.P.; Xie, Y.M. 1998: Evolutionary structural optimisation using a bi-directional algorithm. *Eng. Comp.* **15**, 1031–1048

Rodrigues, H.; Fernandes, P. 1995: A material based model for topology optimization of thermoelastic structures. *Int. J. Numer. Meth. Engrg.* **38**, 1951–1965

Rozvany, G.I.N.; Bendsøe, M.P.; Kirsch, U. 1995: Layout optimization of structures. *Appl. Mech. Rev.* **48**, 41–118

Sigmund, O.; Torquato, S. 1997: Design of materials with extreme thermal expansion using a three-phase topology optimization method. *J. Mech. Phys. Solids* **45**, 1037–1067

Sigmund, O.; Petersson, J. 1998: Numerical instabilities in topology optimization: A survey on procedures dealing with checkerboards, mesh-dependencies and local minima. *Struct. Optim.* **16**, 68–75

Swan, C.C.; Kosaka, I. 1997: Voigt-Reuss topology optimization for structures with linear elastic material behaviours. *Int. J. Numer. Meth. Engrg.* **40**, 3033–3057

Xie, Y.M.; Steven, G.P. 1993: A simple evolutionary procedure for structural optimization. *Comp. & Struct.* **49**, 885–896

Xie, Y.M.; Steven, G.P. 1996: Evolutionary structural optimization for dynamic problems. *Comp. & Struct.* **58**, 1067–1073

Xie, Y.M.; Steven, G.P. 1997: *Evolutionary structural optimization*. Berlin, Heidelberg, New York: Springer

Youn, S.K.; Park, S.H. 1997: A study on the shape extraction process in the structural topology optimization using homogenization material. *Comp. & Struct.* **62**, 527–538

Zhao, C.; Steven, G.P.; Xie, Y.M. 1997: Evolutionary natural frequency optimization of two-dimensional structures with additional non-structural lumped masses. *Eng. Comp.* **14**, 233–251

Zhou, M.; Shyy, Y.K.; Thomas, H.L. 2000: Checkerboard and minimum member size control in topology optimization. *Proc. WCSMO-3, 3rd World Cong. of Structural and Multidisciplinary Optimization* (held in Buffalo, NY, May 1999). CD-Rom. Also: 2001, *Struct. Multidisc. Optim.* **21**, 152–158